Thermally induced lineations on the asteroid Eros: Evidence of orbit transfer

Andrew J. Dombard and Andrew M. Freed[1]

Department of Terrestrial Magnetism, Carnegie Institution of Washington, Washington, DC, USA

Received 20 March 2002; revised 7 May 2002; accepted 9 May 2002; published 31 August 2002.

[1] Several systems of tectonic lineations have been observed on the surface of the asteroid 433 Eros. We suggest that many of these lineations may have resulted from thermal stresses associated with a secular change in surface temperature due to orbit migration. We demonstrate how thermal diffusion can lead to tectonic features and how such features should be oriented with respect to Eros' complex geometry. Comparison to observed lineations suggests that some may be explained by thermal stresses. Such stresses represent a largely unexplored tectonic process on asteroids and could be used to gain rare insight into chaotic orbital dynamics. If correct, our results imply a gross orbital history over the last ~100 Myr involving slow (>several Myr), inward migration followed by more rapid, outward migration to its present orbit. *INDEX TERMS:* 6205 Planetology: Solar System Objects: Asteroids and meteoroids; 5475 Planetology: Solid Surface Planets: Tectonics (8149); 6040 Planetology: Comets and Small Bodies: Origin and evolution; 3210 Mathematical Geophysics: Modeling

1. Introduction

[2] While in orbit around 433 Eros, NASA's Near Earth Asteroid Rendezvous (NEAR)-Shoemaker spacecraft returned images that revealed a pervasive network of lineations (Figure 1). An irregularly shaped asteroid, Eros measures ~34 × 11 × 11 km, and its large-scale shape is dominated by three features, most likely impact related: an ~10 km wide, saddle-shaped depression called Himeros, a flanking depression called Shoemaker Regio, and a 5.3 km diameter crater, Psyche [*Veverka et al.*, 2000; *Robinson et al.*, 2001; *Prockter et al.*, 2002]. The most notable lineation is Rahe Dorsum, a prominent ridge complex that spans about half the asteroid. In addition, there is a global network primarily composed of sinuous to linear depressions, whose members often subtend several tens of degrees and indicate a regional, if not global, formation mechanism. These grooves have a muted appearance, indicative of fractures blanketed by a regolith of the order of ~100 m thick [*Prockter et al.*, 2001a, 2002]. The presence of this global structural fabric suggests that Eros has some degree of internal strength [*Robinson et al.*, 2001; *Prockter et al.*, 2002].

[3] The origin of these lineations is enigmatic, although the large variation in directions and relative ages suggests many different formational events [*Robinson et al.*, 2001; *Prockter et al.*, 2002]. An association with structure within Eros (e.g., planar layering obtained when Eros was a member of a larger, parent body) is not readily apparent. Although the lineations show no obvious link to impact craters [*Prockter et al.*, 2002], the most prevalent interpretation of the groove network is fracture opening during Eros' long collisional history [e.g., *Veverka et al.*, 2000; *Prockter et al.*, 2001a; *Robinson et al.*, 2001]. Rahe Dorsum's morphology suggests compressive tectonism; it and possible tensile features on the other side of Eros may mark a plane cutting through the asteroid [*Prockter et al.*, 2001b].

[4] Here, we propose that some of the lineations may be the product of stresses created by differential thermal expansion due to propagation of a thermal pulse. Such a pulse could result from a secular change in average surface temperature that accompanies chaotic orbit transfer. Indeed, Eros does appear to have undergone orbit transfer, to arrive at its current orbit with a semi-major axis of 1.46 AU. Its spectral class (S) and its observed crater population suggest an origin and long residence in the inner asteroid belt (~2–2.5 AU) [*Veverka et al.*, 2000; *Chapman et al.*, 2002]. Furthermore, dynamical simulations indicate that the orbit of Eros is chaotic on million year time scales, displaying large variations in orbital elements over times as short as millennia [*Michel et al.*, 1998]. While thermal stresses have been suggested as influencing the large-scale shape of asteroids [*Ruangthaveekoon and Germanovich*, 2000] or as responsible for the break-up of comets [*Tambovtseva and Shestakova*, 1999], such stresses represent a mostly unexplored source of tectonism on asteroids.

2. Methods

[5] As orbital histories are not available, we assume that the semi-major axis linearly decreases by a factor of 2, roughly the factor between the orbits of near-Earth and asteroid belt objects. As planetary surface temperatures inversely scale with the square root of distance from the Sun [e.g., *Hartmann*, 1999], the diurnally and annually averaged surface temperature, T_s, is thus given as

$$T_s(t) = T_{s,o}/\sqrt{1 - 1/2t/t_{ot}} \tag{1}$$

where t_{ot} is the orbit transfer time and $0 \leq t \leq t_{ot}$. We assume that Eros began at an initial isothermal temperature of –100°C. The surface then uniformly rose to T_s = –25°C in accordance with (1), corresponding to a present semi-major axis half that of the initial orbit. The speed at which an asteroid equilibrates to the warmer T_s is controlled by thermal diffusion [*Turcotte and Schubert*, 1982]. We

[1] Now at Berkeley Seismological Laboratory, University of California, Berkeley, CA, USA.

0094-8276/02/2002GL015181$05.00

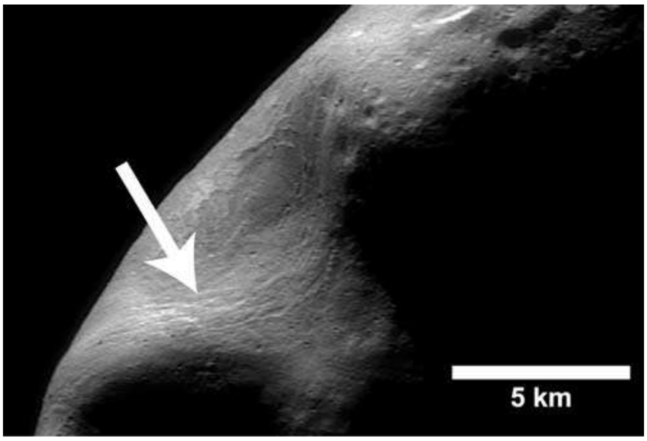

Figure 1. Near Earth Asteroid Rendezvous-Shoemaker spacecraft image of Eros (NASA Image #PIA02469). Himeros is the large, saddle-shaped depression in the image center; to its lower left lies another depression called Shoemaker Regio, in shadow. A segment of Rahe Dorsum is seen on the far side of Himeros, while a modestly coherent cluster of grooves is viewed draping over the left flank of Himeros (highlighted with an arrow).

average annual and diurnal cycles in T_s, because penetration of such high frequency waves will be <10 m and will not likely have regional effects.

[6] To build an intuition, we initially consider a thermoelastic finite element model of a sphere. In principle, such a system could be solved using a series of analytic solutions [*Timoshenko and Goodier*, 1951], although a numerical technique is employed, as we will progress to more complex systems. We use the finite element code MSC.MARC (see http://www.marc.com). This code has been used to investigate other geophysical systems [e.g., *Dombard and McKinnon*, 2000]; benchmarking to analytic solutions and other finite element packages invariably has yielded excellent results. Here, we assume symmetry boundaries conditions, enabling us to conduct calculations in one quadrant of a circular mesh, 6 km in radius. As the bulk behavior of asteroids is not known for certain, we further assume uniform material parameters selected to be consistent with rocky materials [*Turcotte and Schubert*, 1982]: an elastic Young's modulus of 65 GPa, a Poisson's ratio of 0.25, a linear coefficient of thermal expansion of 10^{-5} C^{-1}, and a thermal diffusivity of 10^{-6} m^2 s^{-1}. A conductive time scale (approximately the radius squared over the thermal diffusivity) is $\sim$1 Myr. Certain effects, such as cold, transient creep and the well-fractured nature of Eros, may conspire to lower the effective, bulk elastic moduli, resulting in smaller stresses. Supposing more rapid orbit change can compensate this effect.

3. Results

[7] Figure 2a shows surface horizontal (tangential) stresses and central (radial and tangential) stress (tension is positive) as a function of time, for two different t_{ot} (1 Myr and 5 Myr). Principal stresses are tensile and equal at the sphere's center. Radial stress decreases with distance from the center, reaching zero at the surface; however, tangential stresses decrease more rapidly with distance from the center, becoming compressive as the surface is approached. Because of spherical symmetry, these surface stresses have no preferred orientation. Stress reaches a maximum when orbital transfer is completed, i.e., when the surface-interior temperature differential is largest, and then decay back to zero as temperatures within the sphere equilibrate. Temperature differentials and stress magnitudes are larger for shorter t_{ot}. The mechanics are identical for a secular decrease in T_s; however, the stress regimes are reversed.

[8] The reduction of stresses associated with thermal equilibrium occurs because the sphere is mechanically elastic. If thermal stresses were sufficient to induce faulting before orbital transfer is achieved, however, then stresses would not revert back to a zero stress state as thermal equilibrium is regained. To investigate the influence of faulting on the cycle of thermal stresses, we add von Mises plasticity, a continuum approximation of discrete, brittle failure, to our simulations (as gravitational overburden

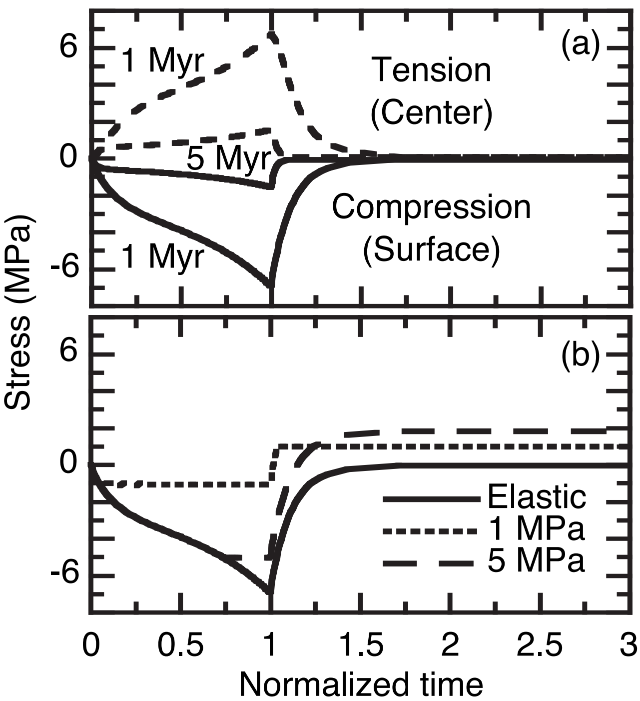

Figure 2. (a) Plot of surface horizontal (tangential) stresses (solid curves) and central (radial and tangential) stress (dashed curves) in a spherical, elastic asteroid as a function of time, normalized by the orbit transfer time. Results are shown for two orbit transfer times: 1 Myr and 5 Myr. Increasing surface temperature creates surface compression and interior tension. Stress magnitudes are greater for shorter transfer times and then decay as the asteroid thermally equilibrates. (b) Plot of surface horizontal stresses in a spherical asteroid as a function of time, normalized by the transfer time of 1 Myr. Results are shown for an elastic case and for two cases that include plasticity with cohesions of 1 MPa and 5 MPa. Here, plastic failure limits the loading stresses. Consequently, unloading stresses associated with thermal equilibration exceed the loading stresses, reversing the stress regimes. For sufficiently low cohesions, excess unloading stresses can also induce failure.

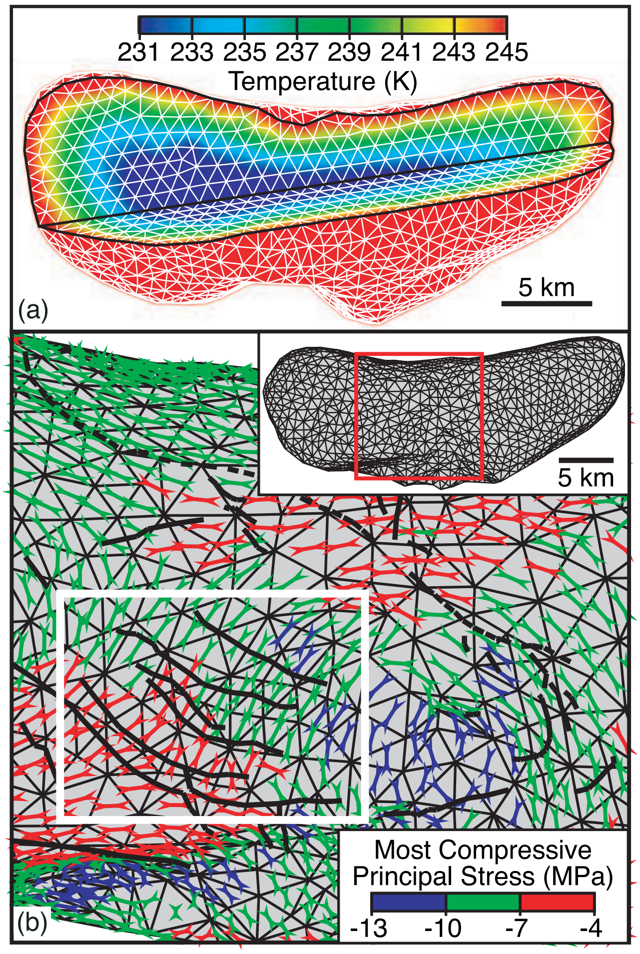

Figure 3. (a) Cutaway view of the finite element mesh of Eros, along with temperatures calculated at the orbital transfer time of 1 Myr. The maximum temperature differential is ~19 K; the color scheme is limited and is selected to highlight the variation in temperature between the surface and the interior. (b) Calculated most compressive principal stress directions and magnitudes (compression is negative) based on the temperature differentials shown in Figure 3a. The portion of the Eros surface as outlined by the red box is shown in the inset. Observed lineations (thick black lines), particularly the prominent cluster highlighted in Figure 1 (white box), tend to run perpendicular to these stress directions, suggesting that such lineations may have a thermal stress origin. Rahe Dorsum (dashed black lines) often trends parallel to the predicted stress directions, suggesting that this ridge complex did not originate from thermal stresses.

stresses in an ~10 km sized asteroid are likely less than ~10^{-1} MPa, we implement a plastic failure criterion independent of hydrostatic stress). We simulate two cases, one with a cohesive strength of 1 MPa, and one with a strength of 5 MPa, both reasonable for a heavily fractured asteroid that exhibits some global strength.

[9] Results of our elastoplastic calculations are shown in Figure 2b for the case of t_{ot} = 1 Myr. As in the elastic case, an increase in T_s initially produces a compressive stress regime near the surface and an interior tensile regime, although plastic failure limits stress magnitudes. Compressive tectonic features would be formed during this phase. When temperature equilibrates after t_{ot}, the stress state does not return to zero, as in the elastic case, but overshoots, inducing a tensile tectonic environment. The overshoot occurs because unloading stresses are now larger than the loading stresses, as faulting limited the latter. Furthermore, the extra unloading stresses may exceed the yield strength again, as in the 1 MPa cohesion case, forming stratigraphically higher, tensile tectonic features. As in the elastic case, the mechanics are similar under a decrease in T_s, although the sign of the stress regimes and the resultant stratigraphy would be reversed. Thus, for a single change in T_s, both compressive and tensile tectonic features may be generated.

[10] Surface stresses for a spherical asteroid are horizontally isotropic, yielding tectonic features with no preferred orientation. Conversely, tectonic features resulting from spatially non-uniform surface stresses will, in general, trend perpendicular to the most compressive/tensile principal stress direction in a compressive/tensile regime. The complex shape of Eros guarantees that thermal stresses will not be horizontally isotropic. To determine how its shape may influence thermal stresses, we develop a fully three-dimensional model of Eros, possessing ~17,000 elements, using the I-deas finite element package (see http://www.eds.com), with the mesh geometry determined by the NEAR-Shoemaker Laser Rangefinder experiment [*Zuber et al.*, 2000]. Like the MARC package, I-deas has been used to investigate other geophysical systems [e.g., *Freed and Lin*, 2001] and is well benchmarked. Material parameters and profiles in T_s are the same as in the t_{ot} = 1 Myr, spherical case, although as our main concern is with stress orientations, we neglect plasticity, which primarily limits stress magnitudes.

[11] Figure 3a shows a cutaway view of the mesh, along with temperatures at t_{ot}. The maximum surface-interior temperature differential is ~19 K and gives rise to compressive surface differential stresses that can exceed 10 MPa (Figure 3b), which is likely sufficient to initiate faulting. Figure 3b also shows the orientations of the calculated, most compressive principal stress directions and of several observed lineations, taken from a preliminary geologic map [*Veverka et al.*, 2000]. The lineations are, in general, perpendicular to these stress directions, and are thus reasonably consistent with a thermal stress origin. The best positive correlation is found with perhaps the most coherent cluster of lineations in this preliminary map (see Figure 1), a set of ~6 grooves flanking the edge of Himeros (outlined by the white box in Figure 3b). The most notable exception is Rahe Dorsum (dashed black lines in Figure 3b); more often than not, it lies parallel to the most compressive principal stress.

4. Discussion

[12] While the agreement between predicted and observed orientations is compelling, many assumptions in this analysis are poorly constrained. For instance, thermal stresses are inherently low strain phenomena, and it is unclear how such lineations would be expressed. The subtle morphology of the lineations suggests blanketing by a regolith [*Prockter et al.*, 2001a, 2002]; if true, the amount of opening of a fracture can be estimated by assuming volume conservation

of the draining regolith. Using maximum dimensions of the grooves [*Veverka et al.*, 2000; *Prockter et al.*, 2002] and assuming the fracture propagates to depths of at least several kilometers (consistent with this thermal stress model), fracture displacement is less than ~1 m. The surface expression will be much wider, as the observed width scales more strongly with regolith thickness [*Horstman and Melosh*, 1989]. With a maximum path around Eros approaching 100 km, a differential temperature of order 10 K yields total thermal displacements across the surface of up to 10 m. If this displacement is accommodated by a finite number of features, then the low-strain, thermally induced lineations may be observable. For 100 accommodating fractures, displacement across an individual fracture approaches ~0.1 m, while the effect on the draining regolith may be amplified by collapse of pore spaces. This explanation for reconciling low strains with observed grooves is somewhat *ad hoc* but plausible. Ultimately, the viability of this model will lie in how well predicted stress orientations agree with lineations from a more complete geologic map of Eros.

[13] Alternatively, a common interpretation of grooves on Eros, as well as those seen on Phobos, Gaspra, and Ida, is impact fracturing [*Thomas et al.*, 1979; *Asphaug and Melosh*, 1993; *Veverka et al.*, 1994; *Asphaug et al.*, 1996], although the grooves on Eros do not appear directly linked to craters. Detailed modeling of the cratering process [e.g., *Asphaug et al.*, 1996] on Eros is required to better understand a potential link. Conversely, thermal stress directions tend to encircle large topographic lows, producing radial features (see Figure 3b). Thus, some of the lineations near Psyche and Himeros [*Prockter et al.*, 2001a, 2002] could be due to thermal stresses. Indeed, a complex interplay between thermal stresses and impact fracturing probably exists and may account for a discrepancy between the low-strain nature of thermal stresses and the observed lineations. Moreover, multiple modes of formation may explain the apparent presence of several groove generations [*Robinson et al.*, 2001; *Prockter et al.*, 2002].

[14] Future thermal stress simulations will also need to consider the effects of a variable thickness regolith of low diffusivity material, as well as incorporate surface temperatures that account for the rotational and orbital geometry of Eros. These factors can affect how heat diffuses into the body and thus may change the pattern of lineations between different orbital migration events. As these properties, particularly the orbital factors, may change between (and during) migration episodes, this possibility is yet another avenue by which several generations of lineations may be created. Other simulations will consider the effects of asteroid-cutting fracture planes, which may be marked by Rahe Dorsum. Future analyses will also benefit from more detailed geologic maps based on NEAR-Shoemaker results.

[15] We have demonstrated that many of the lineations on Eros may be consistent with a thermal stress origin. Besides providing a possible explanation for the genesis of tectonic features on what has been expected to be a largely tectonically inert object, our results imply a possible sequence for the evolution of Eros' orbit. Given the prevalence of grooves (presumably tensile features) and the dearth of compressive features, we can infer that Eros experienced an inward migration too slow (several Myr or greater) to produce observable compressive features, overshooting its present orbital position. This inward migration was then followed by a rapid (less than ~1 Myr) outward migration, cooling the asteroid fast enough to create tensile surface features. This path is roughly consistent with orbital histories determined from dynamical simulations [*Michel et al.*, 1998]. Thus, study of thermally induced lineations could conceivably be used to constrain orbital histories, illuminating the chaotic dynamics of near-Earth asteroids.

[16] **Acknowledgments.** This research has been supported by the NASA Planetary Geology and Geophysics Program under grants NAG5-4077 and NAG5-10165. We thank Maria Zuber, Andrew Cheng, and Olivier Barnouin-Jha for supplying the coordinates of the Eros plate model. Discussions with Rebecca Ghent and Louise Prockter were helpful, while suggestions by Jonathan Aurnou, Steven Hauck, Jay Melosh, and Sean Solomon helped improve this manuscript. We also thank Erik Asphaug and Olivier Barnouin-Jha for insightful reviews.

References

Asphaug, E., and H. J. Melosh, The Stickney impact of Phobos: A dynamical model, *Icarus*, *101*, 144–164, 1993.

Asphaug, E., J. M. Moore, D. Morrison, W. Benz, M. C. Nolan, and R. J. Sullivan, Mechanical and geological effects of impact cratering on Ida, *Icarus*, *120*, 158–184, 1996.

Chapman, C. R., W. J. Merline, P. C. Thomas, J. Joseph, A. F. Cheng, and N. Izenberg, Impact history of Eros: Craters and boulders, *Icarus*, *155*, 104–118, 2002.

Dombard, A. J., and W. B. McKinnon, Long-term retention of impact crater topography on Ganymede, *Geophys. Res. Lett.*, *27*, 3663–3666, 2000.

Freed, A. M., and J. Lin, Delayed triggering of the 1999 Hector Mine earthquake by viscoelastic stress transfer, *Nature*, *411*, 180–183, 2001.

Hartmann, W. K., *Moons and Planets*, 4th ed., p. 297, Wadsworth, Belmont, 1999.

Horstman, K. C., and H. J. Melosh, Drainage pits in cohesionless materials: Implications for the surface of Phobos, *J. Geophys. Res.*, *94*, 12,433–12,441, 1989.

Michel, P., P. Farinella, and C. Froeschlé, Dynamics of Eros, *Astron. J.*, *116*, 2023–2031, 1998.

Prockter, L. M., et al., Structural geology of Eros from NEAR Shoemaker imaging, *Lunar Planet. Sci.*, *XXXII*, CD-ROM abstract #1947, 2001a.

Prockter, L. M., P. C. Thomas, M. Robinson, and J. Joseph, Evidence for global structure within 433 Eros (abstract), *Eos Trans American Geophysical Union*, *82*(47), 711, Fall Meet. Suppl., 2001b.

Prockter, L., P. Thomas, M. Robinson, J. Joseph, A. Milne, B. Bussey, J. Veverka, and A. Cheng, Surface expressions of structural features on Eros, *Icarus*, *155*, 75–93, 2002.

Robinson, M. S., P. C. Thomas, J. Veverka, S. L. Murchie, and D. B. J. Bussey, The geology of Eros, *Lunar Planet. Sci.*, *XXXII*, CD-ROM abstract #2134, 2001.

Ruangthaveekoon, C., and L. Germanovich, Thermomechanical mechanism of shape evolution of the Near-Earth Asteroids (abstract), *Eos Trans American Geophysical Union*, *81*(48), 771, Fall Meet. Suppl., 2000.

Tambovtseva, L. V., and L. I. Shestakova, Cometary splitting due to thermal stresses, *Planet. Space Sci.*, *47*, 319–326, 1999.

Thomas, P., J. Veverka, A. Bloom, and T. Duxbury, Grooves on Phobos: Their distribution, morphology, and possible origin, *J. Geophys. Res.*, *84*, 8457–8477, 1979.

Timoshenko, S., and J. N. Goodier, *Theory of Elasticity*, ch. 14, McGraw-Hill, New York, 1951.

Turcotte, D. L., and G. Schubert, *Geodynamics*, Wiley, New York, 1982.

Veverka, J., et al., Discovery of grooves on Gaspra, *Icarus*, *107*, 72–83, 1994.

Veverka, J., et al., NEAR at Eros: Imaging and spectral results, *Science*, *289*, 2088–2097, 2000.

Zuber, M. T., et al., The shape of 433 Eros from the NEAR-Shoemaker Laser Rangefinder, *Science*, *289*, 2097–2101, 2000.

A. J. Dombard and A. M. Freed, Department of Terrestrial Magnetism, Carnegie Institution of Washington, 5241 Broad Branch Rd. NW, Washington, DC 20015, USA. (dombard@dtm.ciw.edu)